IHRT IFAC TU

International Federation of Automatic Control – IFAC

Institute for Handling Devices and Robotics - IHRT
Vienna University of Technology

6th IFAC Symposium on Robot Control

SYROCO '00

September 21st - 23rd, 2000
Vienna, Austria

Preprints

VOLUME I

Edited by:

Peter Kopacek
Institute for Handling Devices and Robotics
Vienna University of Technology

HYBRID POSITION/FORCE ALGORITHMS FOR BIPED LOCOMOTION

Filipe M. Silva[*] and J.A. Tenreiro Machado[**]

[*] *Dept. of Mechanical Engineering, University of Aveiro, Portugal*
[**] *Dept. of Electrical Engineering, Polytechnic Institute of Porto, Portugal*

Abstract: This paper addresses the problem of modelling and control of a biped robot by combining Cartesian-based position and force control algorithms. The complete walking cycle is divided in two phases: *i*) single support - in which it is studied the trajectory controllability based on simple motion goals and *ii*) exchange of support - in which the forward leg should absorb the impact and then gradually accept the robot's weight. The contact of the foot with the constrained surface is modelled through linear spring-damper systems. The control algorithms are simulated and their effectiveness and robustness are discussed.

Keywords: trajectory planning, dynamics, control algorithms, force control, walking

1. INTRODUCTION

Nowadays, several aspects of modern life involve the use of intelligent machines capable of operating under dynamic interaction with its environment. The field of biped locomotion is representative of this interest concerning human-like robots. A growing community of researchers is working towards a better understanding of machines that can balance, strike purposively and coordinate multiple degrees of freedom (Hirai, *et al.*, 1998; McGeer, 1990; Raibert, 1986; Yamaguchi, *et al.*, 1994). The major problems associated with the analysis and control of bipedal systems are the high-order, highly coupled nonlinear dynamics and, furthermore, the discrete changes in the dynamic phenomena due to the nature of the walking gait. At the same time, the degree of freedom formed between the foot and the ground surface is unilateral and underactuated (Goswami, 1999).

This paper addresses the problem of modelling and control of a biped robot by combining Cartesian-based position and force control algorithms. The aim of the present study is to propose algorithms that make the robot able to adapt to changes in the dynamical interaction with the environment.

In this line of thought, the remainder of the paper is organised as follows. Section 2 describes briefly the biped model and the motion planning problem. Section 3 is dedicated to control issues and the associated strategies. Section 4 studies the application of the proposed algorithms and presents simulation results. Section 5 concludes this paper and outlines the perspectives towards future research.

2. BIPED MODEL

Figure 1 shows the planar biped model that consists of body, thigh, shank and feet. The model considers ideal actuators at all joints including the ankles. In this study, it is assumed that a complete walking cycle is divided in:

i) Single-support phase (SS), in which one leg is in contact with the ground and the other leg swigs forward.
ii) Double-support phase (DS), in which the legs trade role.

The equations describing the motion of the biped robot include the conditions of non-contact and contact with the environment. The redundancies in the exchange of support are used to satisfy the torque continuity when the two legs trade role.

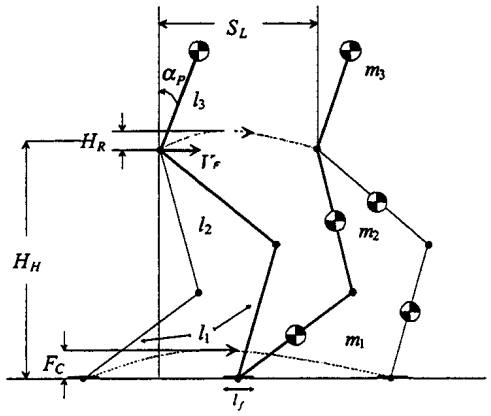

Fig. 1. Planar biped model.

2.1 Motion Planning

The motion planning is accomplished by prescribing the Cartesian trajectories of the body and the lower extremities of the leg. First, the biped motion is characterised in terms of a set of locomotion variables, such as step length S_l, hip height H_h, hip ripple H_r, hip pitch angle α_p, foot clearance F_c and forward velocity V_f (Figure 1). Then, the trajectory generator synchronises and coordinates the legs using cycloid profiles and other sinusoidal time functions.

2.2 Performance Evaluation

In this section, we establish the correlation among the above locomotion variables and some important aspects of walking, such as power efficiency, foot rotation and torque discontinuities. The present analysis explores the single support phase for a total system mass of $M = 70kg$ and body height of $L = 1.8m$ (Table 1).

Table 1 The robot link lengths and masses.

i	$l_i(m)$	$m_i(kg)$
1	0.5	4.0
2	0.5	7.5
3	0.3	47

Power Index The power cost function is obtained by averaging the motor electrical losses over a period T:

$$L_e = \frac{1}{T}\int_0^T \tau^T \tau \, dt \qquad (1)$$

where τ is the n-vector of joint torques.

A complete analysis of the power performance can be found in other articles by Silva, *et al.* (1999). To minimise the average power lost L_e the hip height must be about 95% of the total height, with step lengths in the range of $0.2 \le S_l \le 0.5m$ (with a constant $V_f = 1.0ms^{-1}$).

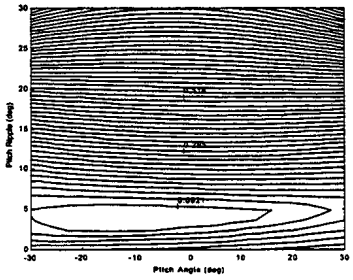

Fig. 2. Mean CoP point F_r vs. P_a and P_r.

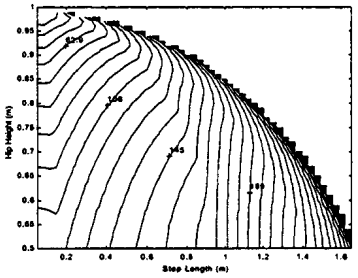

Fig. 3. Mean absolute discontinuity S_m vs. S_l and H_h.

Foot Stability Index The rotational equilibrium of the foot is the major factor of postural instability in legged robots. In this sense, the active control of the centre of pressure (CoP) may be of major importance. At this stage, we simplify this issue by simply monitoring the CoP state. Consequently, it is defined a global index F_r as the average, over on cycle, of the distance between the CoP point P and the ankle O:

$$F_r = \frac{1}{T}\int_0^T \left|\overline{OP}\right| dt \qquad (2)$$

In this way, it can be estimated the necessary foot length to avoid foot rotation. The results plotted in Figure 2 shows the influence of the pitch angle α_p in the evolution of the CoP. From these values and analysing the CoP variation during the cycle, we conclude that it is required a foot length $l_f = 0.3m$.

Torque Discontinuity Index Since the support shifts instantaneously from one limb to the other, the torque variables are discontinuous at the instant of support exchange (t_c). This justifies the definition of the index S_m defined as the sum of the absolute joint torque discontinuities. The contour plot (Figure 3) gives some hints to select the S_l and H_h.

3. POSITION/FORCE HYBRID CONTROL

The essence of locomotion is to transport the body from an initial position to a desired one throughout the action of the lower limbs. The biped's movement is produced by ideal power actuators and constrained by environmental aspects.

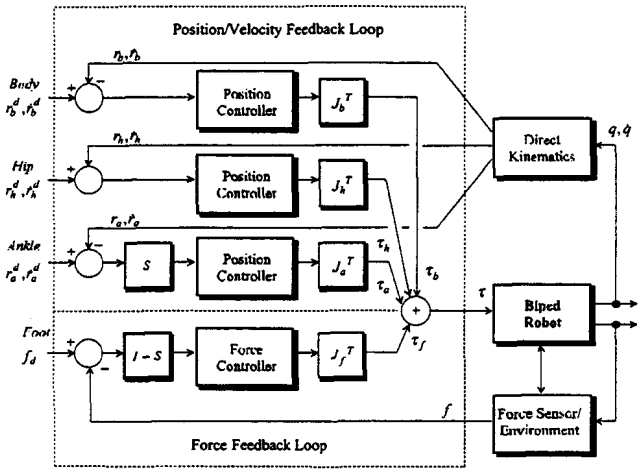

Fig. 4. Hybrid Position/Force Controller.

The resultant motion depends on two factors, namely, the structural and functional characteristics of the intelligent controller and the physical phenomena such as gravity, friction and reaction forces. Bearing these facts in mind, we propose a hybrid position/force controller to achieve Cartesian position/velocity tracking control and force compliance with the ground.

The block diagram of the hybrid control algorithm is shown in Figure 4. The control architecture allows the integration of high level motion goals related with the body, hip and swing foot coordinates. During the single-support, the position/velocity loop assures that the biped follows a planned trajectory, whilst the force control remains off. When the swing foot contacts the environment, additional control efforts are needed to stabilise the robot during the post-impact phase. As a result, the position and force feedback are summed to provide the torque commands:

$$\tau = \tau_b + \tau_h + \tau_a + \tau_f \qquad (3)$$

where τ_b, τ_h, τ_a are the body, hip and ankle components acting in the position subspace, and τ_f is the command acting in the force subspace. The control performance requirements are simultaneously satisfied, both for the desired position and force trajectories. At the same time, the control laws are designed independently: the position control law consists of a PD action (fast response) and the force control law consists of a PI action (small steady-state errors).

3.1 Controllability Analysis in the SS Phase

In this section we will focus on the single-support phase while ignoring the events of impact and transfer of support. Moreover, the goal of postural stability is achieved by an appropriate motion planning and it is not included in the control algorithm. Hence, the discussion will be limited to trajectory stability considerations. The Cartesian-based PD position controller uses the transpose Jacobian matrix to generate the output torque commands.

The main problem is the selection of the individual contributions that provide coordinated gaits and a steady dynamic walking. On the other hand, the performance imposed by the task to be accomplished (*e.g.*, normal walking, fast walking, climb stairs or sloped surfaces) shall dictate the importance of each component. This study will be limited to exploring the implications of the body, hip and swing foot in normal walking. Based on these coordinates, we are able to provide high level motion goals, such as: *i*) to maintain a constant forward velocity or to apply a horizontal oscillation; *ii*) to maintain a constant hip height or to apply a desired vertical oscillation; *iii*) to place the foot on the ground with zero velocity.

The system's controllability analysis appears in the form of two performance indexes that can be defined as follows. On one side, by regarding the forward kinematics of the mechanism, we can determine an index based on the statistical average of the well-known mean-square error:

$$\xi_h^p = \sqrt{\frac{1}{T}\int_0^T \left[\left(x_h^d - x_h\right)^2 + \left(y_h^d - y_h\right)^2\right]} \qquad (4)$$

$$\xi_h^v = \sqrt{\frac{1}{T}\int_0^T \left[\left(\dot{x}_h^d - \dot{x}_h\right)^2 + \left(\dot{y}_h^d - \dot{y}_h\right)^2\right]} \qquad (5)$$

Here, x_h^d, y_h^d and x_h, y_h are the desired and real hip positions, respectively, and $\dot{x}_h^d, \dot{y}_h^d$ and $\dot{x}_h, \dot{y}_h$ are the corresponding velocities. On the other side, it is measured the swing foot velocities, $\dot{x}_a^-$ and $\dot{y}_a^-$, immediately before the impact occurs at $t = t_s$.

The desired goals are decomposed into horizontal and vertical directions as described in Table 2. From the results, it seems that the controller is able to adapt well in accordance with the desired goals. However, the minimisation of the impact velocities can be a problem given their significant variations. In practical terms, this implies that the robot should incorporate some kind of actively controlled compliant mechanism under their feet (similar to the Achilles tendon and the arch of the foot).

Table 2 Goal definition and performance of the controller.

Desired Goals	X direction			Y direction			Performance	
	Hip	Body	Ankle	Hip	Body	Ankle	ξ_h^p, ξ_h^v	$\dot{x}_a^-, \dot{y}_a^-$
Pos.	0	0	0	1	1	0	1.9e–2	2.6e–3
Vel.	1	1	1	0	0	1	3.2e–2	7.5e–2
Pos.	0	0	1	1	1	1	1.3e–3	7.5e–6
Vel.	1	1	1	0	0	1	4.7e–3	1.0e–4
Pos.	0	1	1	1	1	1	4.6e–5	1.3e–5
Vel.	1	1	1	0	1	1	3.8e–4	1.1e–3
Pos.	1	1	0	1	1	0	3.8e–5	2.6e–3
Vel.	1	1	1	1	1	1	7.8e–3	8.8e–2
Pos.	1	1	1	1	1	1	1.2e–4	1.5e–5
Vel.	1	1	1	1	1	1	9.3e–4	2.6e–3

3.2 Environment Model and Sensorial Requirement

At each footfall the walking system may suffer impact forces and incur on additional accelerations that influence the forward velocity (Zheng, and Hemami, 1984). Some design objectives are considered in order to reduce the impact effects: *i*) minimisation of the impact velocities; *ii*) zero mass feet. These design factors just reduce the impact effects. Hence, the overall control (including impact and exchange of support) involves the modelling of the environment and the integration of position, velocity and force feedback.

The contact of the swing foot with the constraint surface is modelled through linear spring-damper systems in the vertical and horizontal directions. The tangential and normal reaction forces applied to the foot are computed as:

$$\begin{aligned} f_t &= -B_x\dot{x} - K_x(x - x_0) \\ f_n &= -B_y\dot{y} - K_y y \end{aligned} \tag{6}$$

where B_x, B_y and K_x, K_y are the damping coefficient and the spring stiffness, respectively, and x_0 is the position of the foot at the moment of its initial contact. The parameters of the environment model are summarised in Table 3.

Table 3 Environment parameters.

B_x (*Ns/m*)	K_x (*N/m*)	B_y (*Ns/m*)	K_y (*N/m*)
5000	50000	500	5e6

In order to improve the motion smoothness, the forward leg must absorb the impact energy and, afterwards, the support must be shifted gradually from the trailing to the leading legs. At the same time, the condition of torque continuity (switching phase) implies that the centre of pressure (CoP) underneath the foot must be properly tracked. For that, we assume the existence of two force sensors in the extremities of the foot as illustrated in Figure 5. The contact forces between foot and ground surface must satisfy the pressure condition and the CoP must lie inside the footprint.

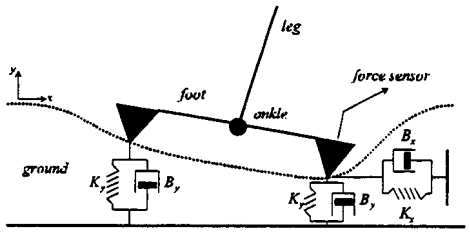

Fig. 5. Constraint environment model.

3.3 Control Strategies

The goal of this section is to describe the most important aspects of the controller implementation. The information flows in the different phases of the walking cycle as depicted in Figure 6 (with impact and switching events). The dynamic selection matrix S determines the subspaces for which force and/or position are controlled. The respective values depend on the particular phase of the walking cycle:

i) during the SS, the swing foot is position controlled and the elements are selected "one".

ii) during the initial phase of the DS, the selection matrix assures a transition period in which the position and force change gradually in opposite directions.

The impact velocities determine the initial conditions that influence to a large extent the transient duration and the overshoots. In this context, it is introduced an enhancement to the PI force controller by adapting its controller gains: *(i)* immediately after the contact the proportional action, in the tangential component, is selected to be zero; *(ii)* the gains are incrementally adjusted after the transient impact to minimise steady-state errors.

Each joint is acted by several torque components that may generate either summing or subtracting terms. Therefore, at the end of the switching phase, position and force are activated simultaneously in opposite directions, meaning a low net torque.

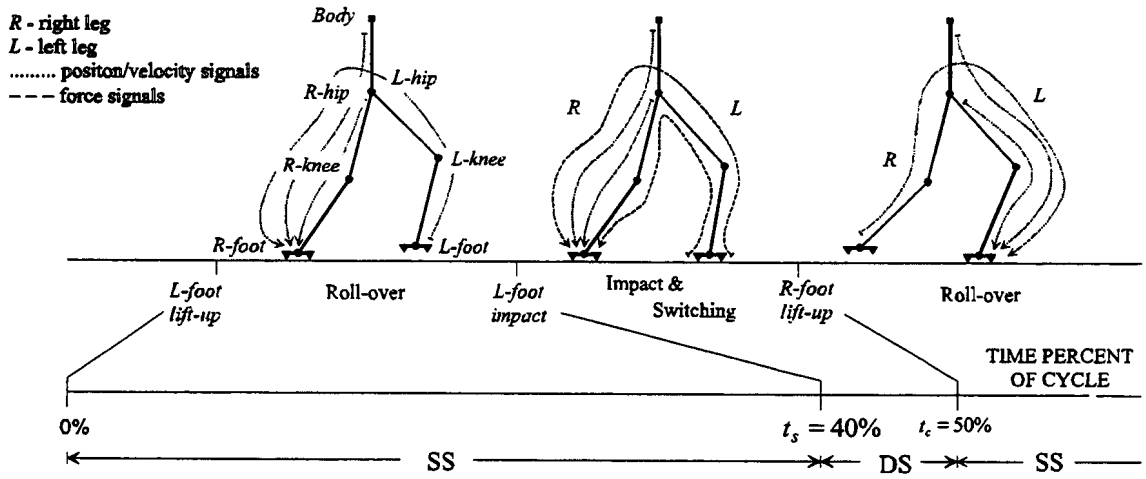

Fig. 6. Controller activity and information flow during half a cycle.

4. SIMULATION RESULTS

When the motion of the biped robot is selected according to given performance criteria (*e.g.*, minimal lost power), the effects of the planned reference trajectories are usually not evident, because their merits or drawbacks may be overridden by the controller's actions. Nevertheless, an adequate motion planning can still ease the controller efforts and helps the execution of the locomotion process. For example, when the biped robot prepares to contact with the ground surface, movements with small effective inertias can be used in advance to reduce the impact forces. Bearing this in mind, the simulations are carried out assuming the locomotion variables in Table 4.

Table 4 Locomotion variables.

$S_l\,(m)$	$H_h\,(m)$	$H_r\,(m)$	$\alpha_p\,(deg)$	$F_c\,(m)$	$V_f\,(m/s)$
0.4	0.95	0.0	5.0°	0.02	1.0

To illustrate the control strategies, the biped robot is simulated along a complete walking cycle for a sampling controller frequency $f_c = 10KHz$. We assume that: *i*) the biped starts the movement $t = 0$ with the lift off the ground of the rear foot; *ii*) the swing foot strikes the ground at $t_s \approx 0.35s$; and *iii*) the support transition occurs at $t_c = 0.4s$. The foot reference trajectory (Figure 7) is selected with the objective of keeping the magnitude of the impact force as small as possible. The computed individual joint torques are depicted in Figure 8. From these charts, we conclude that the controller is effective to regulate the impact transitions.

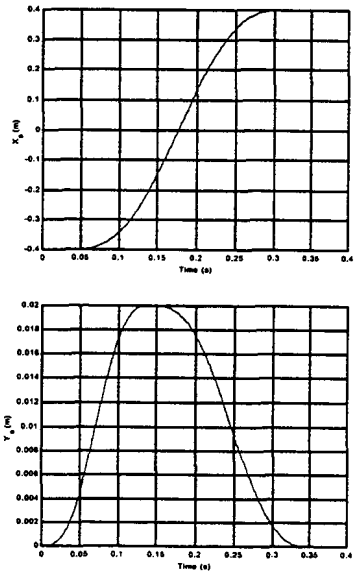

Fig. 7. Reference trajectory of the swing foot.

At the same time, the application of the direct force feedback algorithm solves the force distribution problem and assures continuous torques. The smooth transfer of weight (Figure 9(*a-b*)), is accomplished through a linear time evolution. Part of the oscillatory behaviour, before the impact at t_s and after the support transition at t_c, is due to the requirements posed by the planned trajectory of the swing foot. This justifies the inclusion of a non-rigid foot model in the future research. Finally, the effect of the impact on the hip variable is shown in Figure 9(*c*) that reveals a correct x_h displacement and some disturbance on the y_h coordinate.

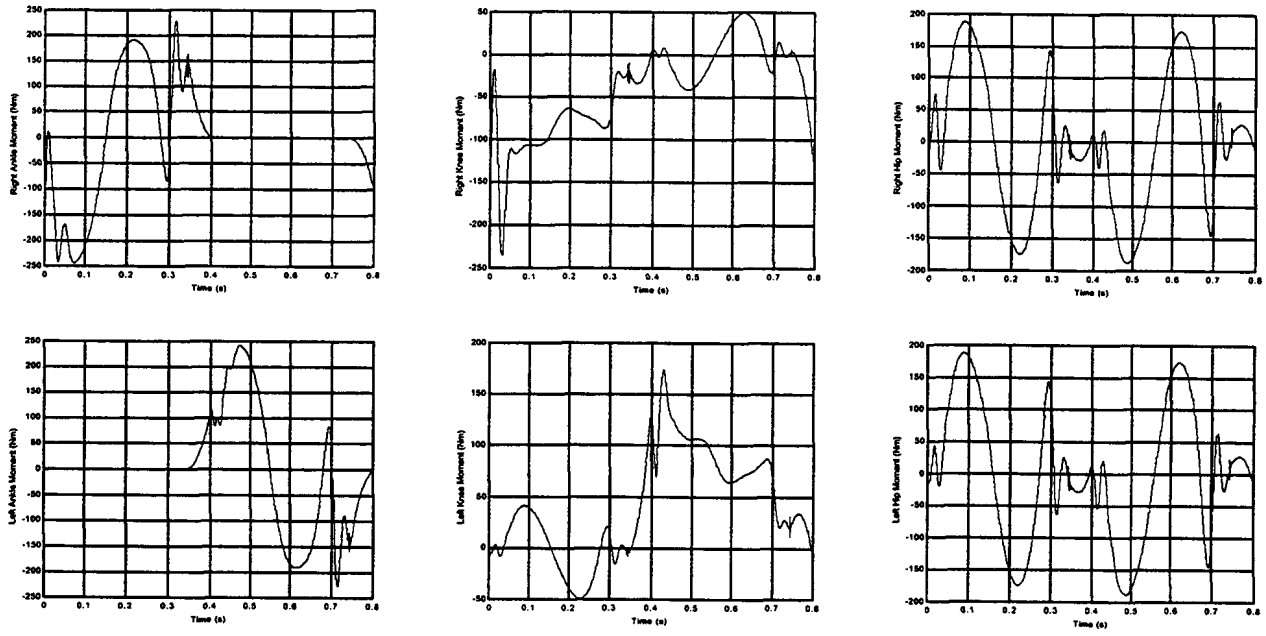

Fig. 8. Ankle, knee and hip torques during one cycle.

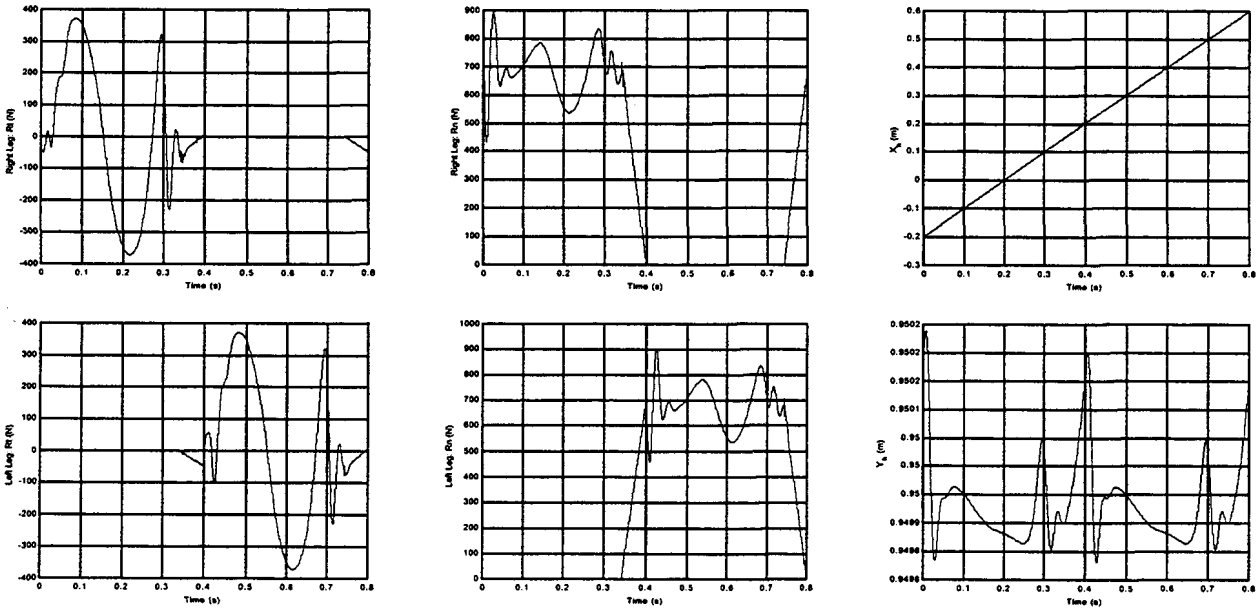

(*a*) (*b*) (*c*)

Fig. 9. (*a*) tangential and (*b*) normal reaction forces on both legs; (*c*) reference and real hip coordinates.

5. CONCLUSIONS

In this paper, we have investigated the combination of position/velocity and force control algorithms. The results suggest three major comments. First, the position controller adapts well to different desired goals. Second, the application of the direct force feedback algorithm allows a smooth transfer of weight. Moreover, an adequate force distribution along the landing foot assures continuous torques. Third, the combination of positional and force information results in a stable contact. However, the system's performance depends strongly on the foot trajectory. This fact suggests the consideration of active compliant feet (*i.e.*, biological-like) with some kind of shock absorption mechanism.

The research should continue in two main directions: *i*) to minimise the dependence on high level planned motions and *ii*) to incorporate a dynamic stability criterion into the control algorithm. In this line of thought, future work will address the refinement of our controller to consider the reaction forces between the feet and the ground in the single-support phase. At the same time, it seems essential to combine fundamental force control techniques with more advanced algorithms such as adaptive control, robust control and learning methods.

ACKNOWLEDGEMENTS

The first author is supported by the *Fundação para a Ciência e a Tecnologia* (FCT) under grant PRAXIS XXI/BD/9541/96.

REFERENCES

Furusho, J. and A. Sano (1990). Sensor-based Control of a Nine-link Biped. *Int. Journal of Robotic Research*, Vol.9, No.2, pp. 83-93.

Goswami, A. (1999). Postural Stability of Biped Robots and the Foot-Rotation Indicator (FRI) Point. *Int. Journal of Robotics Research*, Vol.18, No.6, pp. 523-533.

Hirai, K., M. Hirose, Y. Haikawa and T. Takenaka (1998). The Development of Honda Humanoid Robot. *Proc. IEEE Int. Conf. on R&A*, pp. 1321-1326, Belgium.

Kajita, S. and K. Tani (1996). Experimental Study of Biped Dynamic Walking. *IEEE Control Systems*, pp. 13-19.

McGeer (1990). Passive Dynamic Walking. *Int. Journal of Robotic Research*, Vol.9, No.2, pp. 62-82.

Raibert, M. (1986). *Legged Robots that Balance*, The MIT Press.

Silva, F.M. and J.A. Tenreiro Machado (1999). Energy Analysis During Biped Walking. *Proc. IEEE Int. Conf. Robotics and Automation*, pp. 59-64, Detroit, USA.

Vukobratovic, M. Botovac, D. Surla and D. Stokic (1990). *Biped Locomotion: Dynamics, Stability, Control and Applications*, Springer-Verlag.

Winter, D.A. (1990). *Biomechanics and Motor Control of Human Movement*, John Wiley & Sons.

Yamaguchi, J-I., A. Takanishi and I. Kato (1994). Development of a Biped Walking Robot Adapting to a Horizontally Uneven Surface. *Proc. Int. Conf. on Intelligent Robots and Systems*, pp. 1156-1163.

Zheng, Y.F. and H. Hemami (1984). Impact Effects of Biped Contact with the Environment. *IEEE Trans. Syst. Man Cyber.*, Vol.14, No.3, pp. 437-443.